

Generalized Chudnovsky Algorithm for Real-time PWM Selective Harmonic Elimination/Modulation: Two-Level VSI Example

Ameer Janabi, *Student Member, IEEE*, Bingsen Wang, *Senior Member, IEEE*, and Dariusz Czarkowski, *Member, IEEE*

Abstract—This paper presents a novel approach to significantly reducing the mathematical complexity associated with the selective harmonic elimination (SHE), which allows for the real-time implementation of SHE with a reasonable utilization of the computational power of the digital controller. First, the transcendental equations of the optimization problem are converted to set algebraic equations using Chebyshev polynomials. Second, the set of algebraic equations is reduced to a single univalent polynomial using generalized Newton's identities. The roots of the polynomial hold a unique solution to the optimization problem. We show that the roots of the univalent polynomial can be solved in real-time by direct substitution with no initial guess or iteration. The proposed method is a generalization of a Chudnovsky algorithm; it allows the modulation of the selected harmonics rather than eliminating them. Furthermore, the technique by which the roots of the polynomial are obtained enables one to implement the algorithm in real-time with determinate execution time. This paper lay the groundwork for presenting the generalized algorithm through a two-level voltage source inverter (VSI) drive. More application will follow in the near future.

I. INTRODUCTION

The selective harmonic elimination (SHE) technique effectively reduces the low-order harmonic content of inverter output waveform and generates a high-quality spectrum through the elimination of specific low-order harmonics [1] [2]. Therefore, it has been applied in power electronic controllers extensively, and many related techniques have been proposed in recent years [3]-[6].

The traditional implementation of SHE is to use a lookup table and a modulator driven by a very slow control loop to ensure steady-state stability [7]. Offline SHE implementations share the crucial drawback: the switching angles could not be calculated in real-time and one has to rely on loading the optimal switching angles for each specific modulation index (M_i). During the transient state of a low switching-frequency drive, the low-frequency component of the reference voltage becomes nonsinusoidal [8]. The switching sequence will then be implemented with the optimal angles saved in the lookup table, which is only valid for steady-state conditions. The resulting current dynamic will be far from optimal. Furthermore, there are other sub-transient conditions such as changing the

This paper is an extended version of work published in [1]. We extend our previous work by (a) generalizing the real-time algorithm to modulate the harmonics rather than only eliminating them, (b) introducing the zero crossing detection method to solve the root of the univalent polynomial in determinate real-time, and (c) provide the necessary examples and additional experimental results for large scale validation of the proposed method.

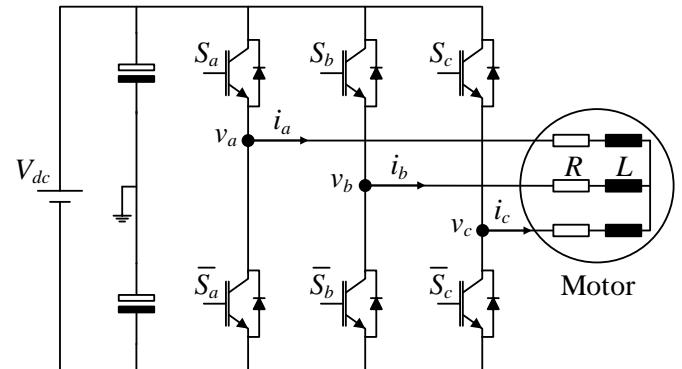


Fig. 1: Two-level voltage source inverter drive.

number of switching events per cycle and changing M_i , which will result in the sub-optimal current performance.

It is important to make the distinction between different types of real-time or online solutions of SHE. Some online SHE algorithms solve the optimization problem in the controller using an iterative process with guessed initial values. Although these methods reduce the memory requirement, they suffer from a poor dynamic performance that is typically inferior to the dynamic performance of the look-up table implementations. For instance, the supposedly real-time method in [9] is unable to perform rapid changes in M_i . It would take 58 ms to change M_i from 0.96 to 0.64. Furthermore, the presented implementation results in larger total harmonic distortion (THD) than the offline solution. Other methods also claim the real-time feature while the solution requires an initial guess and an indeterminate number of iterations [10]. In [11], the switching angles are approximated using curve fitting of the offline solution. Then a carrier waveform is calculated by a cosine function based on the modulation depth. This approach requires saving the curve fitting coefficients for each modulation index. If 1% resolution is desired, it would require 100 polynomials to describe each switching angle. Not to mention that if the switching frequency is changed, a new set of equations is required for each angle. In [12], Chebyshev polynomials are used to convert a set of the transcendental equations into algebraic polynomials. Then the algebraic equations are rearranged through a change of variables to solve for the switching angles. However, the transformation of the transcendental equations is not systematic, and no

generalization was given to simplify the process of transforming the transcendental equations to algebraic equations. The complexity of the derivation increases as the number of the selected harmonics increases. Furthermore, the set of the algebraic equations is solved using inverse cosine function, but the computational effort could be reduced by converting the set of the algebraic equations to a single polynomial. All these drawbacks with the strict operating requirements of high power industrial drives pose serious limitations on the practical viability of the existing approaches.

A new implementation of the real-time selective harmonic elimination (RTSHE) is proposed in this paper. The original contributions of the proposed RTSHE are the following:

1. Presenting the generalized Chudnovsky algorithm. The new algorithm allows modulating the selected harmonics rather than only eliminating them.
2. Presenting a new method of obtaining the values of the optimal switching angles from the polynomial in real-time without resorting to any iterations or guesses.

Preliminary results were published in [1] show that the real-time approach could be a suitable replacement for the conventional offline method. In this article, the authors expand the real-time algorithm to a generalized form without increasing the computational effort. The algorithm is demonstrated through the experiment of the two-level voltage source inverter (VSI) shown in Fig. 1. A comparison between the proposed RTSHE method and the conventional offline method is presented throughout the paper.

The rest of the paper is organized as follows: The proposed RTSHE method is presented in section II. The comparison between the proposed RTSHE and the conventional offline method is presented in section III. The selective harmonic modulation (RTSHM) method is presented in section IV. The experimental results are presented in section V. Finally, the conclusion is presented in section VI.

II. THE PROPOSED REAL-TIME SELECTIVE HARMONIC ELIMINATION

The development of RTSHE starts from manipulating the transcendental equations. Owing to the symmetry of the PWM waveform, only odd harmonics exist. By chopping the PWM waveform n times per quarter cycle, the Fourier coefficients of the odd harmonics are given by

$$b_k = -\frac{4V_{dc}}{k\pi} \left[1 - 2 \sum_{i=1}^n (-1)^{i-1} \cos(k\alpha_i) \right], \quad (1)$$

where k is the harmonic order number $\{1, 3, 5, \dots\}$, n is the total number of the switching angles per quarter fundamental cycle, V_{dc} is the DC-link voltage, and α_i is the optimal switching angle. In SHE, the fundamental component ($k = 1$) is set to a desired amplitude, and the other selected odd harmonics are set to zero. This formulation of the optimization problem leads to the following set of transcendental equations:

$$\begin{aligned} 1 - 2 \cos(\alpha_1) + \dots + (-1)^n 2 \cos(\alpha_n) &= -\frac{\pi b_1}{4V_{dc}} \\ 1 - 2 \cos(3\alpha_1) + \dots + (-1)^n 2 \cos(3\alpha_n) &= -\frac{3\pi b_3}{4V_{dc}} \\ \vdots \\ 1 - 2 \cos(k\alpha_1) + \dots + (-1)^n 2 \cos(k\alpha_n) &= -\frac{k\pi b_k}{4V_{dc}}. \end{aligned} \quad (2)$$

A. Converting the Transcendental Equations to Algebraic Equations:

By using Chebyshev polynomials, the transcendental equations in (2) can be transformed to algebraic equations [13]-[14]. This can be achieved by letting $x_o = \cos(\alpha_o)$ and $x_e = -\cos(\alpha_e)$, where the subscripts o and e denote the odd and even numbers, respectively. This leads to the following set of algebraic polynomials:

$$\begin{aligned} x_1 + x_2 + \dots + x_n &= s_1 \\ x_1^3 + x_2^3 + \dots + x_n^3 &= s_3 \\ \vdots \\ x_1^{2n-1} + x_2^{2n-1} + \dots + x_n^{2n-1} &= s_{2n-1}, \end{aligned} \quad (3)$$

where x_1, x_2, \dots, x_n , hold the solution of the switching angles $\alpha_1, \alpha_2, \dots, \alpha_n$, respectively. $s_1, s_3, \dots, s_{2n-1}$ can be obtained using the proposed recursive algorithm:

$$T_{2n-1}(x)|_{(x^{2n-1}=s_{2n-1})} = \frac{1}{2} + \frac{\pi b_{2n-1}}{8V_{dc}}, \quad (4)$$

where $T_{2n-1}(x)$ is a Chebyshev polynomial of the first kind [15]. This can be found through the recursive formula

$$T_{n+1}(x) = 2xT_n(x) - T_{n-1}(x), \quad (5)$$

where $T_0(x) = 1$ and $T_1(x) = x$. For instance, if the desired fundamental component is set to a specific value b_1 and the rest of the odd harmonics are set to zero, the following values for s can be obtained:

$$\begin{aligned} s_1 &= \frac{1}{2} \left[1 + \frac{\pi b_1}{4V_{dc}} \right] \\ s_3 &= \frac{1}{2} \left[1 + \frac{3\pi b_1}{4V_{dc}} \right] \\ \vdots \\ s_{2n-1} &= \frac{1}{2} \left[1 + \frac{\pi b_1}{4^{n-1}4V_{dc}} \binom{2n-1}{n-1} \right]. \end{aligned} \quad (6)$$

In the case of a three-level VSI such as the neutral point clamped (NPC) inverter [16] or the single phase inverter [17], the following equation can be used to calculate s :

$$s_{2n-1} = \frac{\pi b_1}{4^{n-1}4V_{dc}} \binom{2n-1}{n-1}. \quad (7)$$

The generalized formulas (6) and (7) circumvent the offline recursive derivation effort. The remarkable fact is that the

definition of s becomes explicit, rather than recursive. One can now start the optimization problem from writing down the algebraic polynomials (3) directly, without going through the earlier steps.

B. Converting the Algebraic Equations to a Single Polynomial:

The set of algebraic polynomials in (2) is a symmetric sum of powers. Therefore, it can be further reduced to the following form of the single polynomial using Newton's identities:

$$P(x) = p_0x^n + p_1x^{n-1} + \dots + p_n = 0, \quad (8)$$

where $p_0 = 1$, and p_1 to p_n can be obtained using the generalized version of Newton's identity first presented in [18]. If the series expansion for the desired polynomial is

$$P(x) = \prod_{i=1}^n (x - x_i), \quad (9)$$

then by algebraically manipulating the polynomial terms we get

$$P(x) = x^n \exp\left(-\sum_{m=1}^{\infty} \frac{s_m}{mx^m}\right), \quad (10)$$

where s_m is the power series representation of the polynomials in (3). As in [17], one can eliminate the multiplication x^n term by dividing (10) by $P(-x)$. This leads to the following expression:

$$P(x) = (-1)^n P(-x) G(1/x), \quad (11)$$

where

$$G(1/x) = \exp\left(V(1/x)\right) = \exp\left(-2 \sum_{m=1,3,5,\dots}^{\infty} \frac{s_m}{mx^m}\right). \quad (12)$$

It is possible to analytically express $G(1/x)$ using the generating function approximation:

$$G(x) = g_0 + g_1x + g_2x^2 + \dots = \sum_{n \geq 0} g_n x^n. \quad (13)$$

Generating functions are a single quantity that represents the whole sequence. They were introduced by De Moivre to solve a class of general recurrence problems [19]. We can recover the individual value of g_1, g_2, \dots from $G(x)$ by assuming that the infinite sum (13) exists for some value of x . The exponential term $e^{V(1/x)}$ in (12) can also be represented by the following generating function:

$$V(x) = v_0 + v_1x + v_2x^2 + \dots = \sum_{n \geq 0} v_n x^n. \quad (14)$$

After calculating the values of (13) and (14), each x in the equation will be replaced by its reciprocal to match (12). The coefficients of $G(x)$ can be obtained by using the binomial theorem. However, Euler discovered an efficient method to obtain the power series powers [20]. Consider the following equation:

$$G(x) = e^{V(x)}. \quad (15)$$

By taking the derivative for both sides

$$\frac{dG(x)}{dx} = \frac{dV(x)}{dx} G(x), \quad (16)$$

expanding both sides

$$g_1 + 2g_2x + 3g_3x^2 + \dots = (v_1 + 2v_2x + 3v_3x^2 + \dots)(g_0 + g_1x + g_2x^2 + \dots), \quad (17)$$

rearranging the RHS

$$g_1 + 2g_2x + 3g_3x^2 + \dots = (v_1g_0) + (2v_2g_0 + v_1g_1)x + (3v_3g_0 + 2v_2g_1 + v_1g_2)x^2 + \dots, \quad (18)$$

and by equating the coefficients of the LHS with the RHS, we find that

$$g_n = \sum_{k=1}^n \frac{k}{n} v_k g_{n-k}, \quad (19)$$

where $g_0 = e^{v_0} = 1$. This leads to a simple real-time algorithm by which we can successively determine the coefficients of $G(x)$. To avoid the forbidden abstract way of presenting results, the authors provide the following non-trivial example.

Example: Suppose that for a three-phase voltage source inverter, we are required to eliminate the first three odd harmonics 3rd, 5th, and 7th, and set the modulation index to $0.6283 = \frac{\pi b_1}{4V_{dc}}$. The DC-link voltage is 100V.

The first step is to calculate the value of s for each polynomial in (3) using the proposed generalized formula (6) as follows:

$$s_1 = \frac{1}{2} \left[1 + \frac{0.6283}{4^0} \binom{1}{0} \right] = 0.8141.$$

By plugging in (6) $n = 2, n = 3$, and $n = 4$, we can find that $s_3 = 0.7356, s_5 = 0.6963$, and $s_7 = 0.6718$, respectively. Now the symmetric power sum (3) can be written as

$$\begin{aligned} x_1 + x_2 + x_3 + x_4 &= 0.8141 \\ x_1^3 + x_2^3 + x_3^3 + x_4^3 &= 0.7356 \\ x_1^5 + x_2^5 + x_3^5 + x_4^5 &= 0.6963 \\ x_1^7 + x_2^7 + x_3^7 + x_4^7 &= 0.6718. \end{aligned} \quad (20)$$

The next step is to reduce the system of equation in (20) to a single polynomial of order 4 such that the roots of the polynomial are the values of x_1, x_2, x_3 , and x_4 in (20). Using the expression in (12) for $V(1/x)$, we can calculate the coefficients of the $V(x)$ series as follows:

$$\begin{aligned} V(1/x) &= -2 \sum_{m=1,3,5,\dots}^{\infty} \frac{s_m}{mx^m} \\ &\Rightarrow V(x) = -2 \sum_{m=1,3,5,\dots}^{\infty} \frac{s_m}{m} x^m, \end{aligned}$$

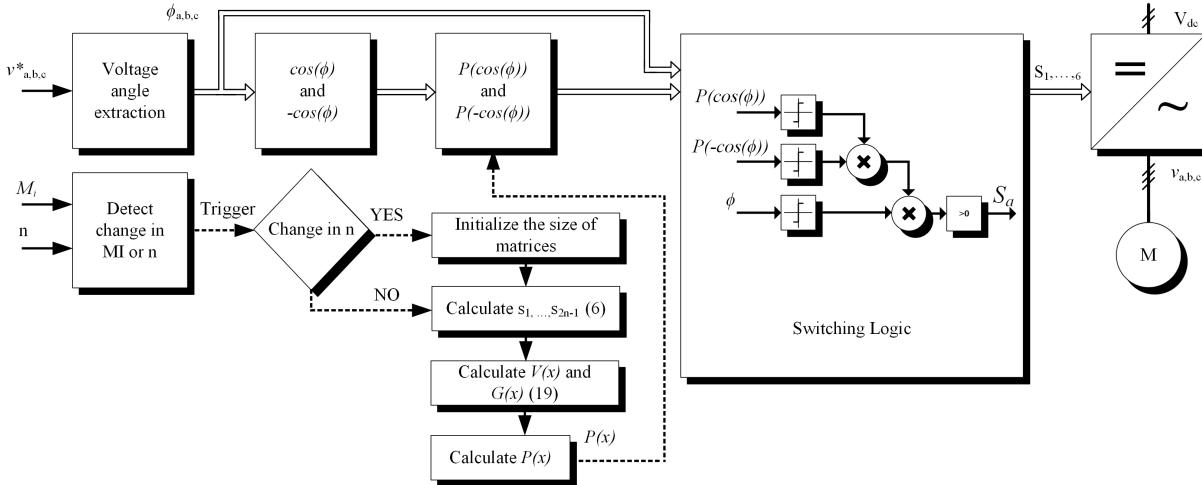


Fig. 2: Illustration of obtaining the value of the optimal switching angles by solving the polynomial in real-time.

where the term $-2\frac{s_m}{m}$ is equal to the coefficient $v_{\frac{m+1}{2}}$ in the generating function (14). s_2, s_4, \dots are set to zero, $v_0=0$. The calculations lead to the following vector:

$$v = [v_0, v_1, v_2, v_3, v_7, v_5, v_6, v_7, v_8]^T = [0, -1.6283, 0, -0.4904, 0 - 0.2785, 0, -0.1919, 0]^T.$$

After obtaining $V(x)$, $e^{V(x)}$ can be calculated using (19), where $g_0 = e^{V(0)} = 1$,

$$g_1 = \sum_{k=1}^1 \frac{k}{1} v_k g_{1-k} = v_1 g_0 = v_1 = -1.6283,$$

$$g_2 = \sum_{k=1}^2 \frac{k}{2} v_k g_{2-k} = \frac{1}{2} v_1 g_1 + \frac{1}{2} v_2 g_0 = \frac{1}{2} (-1.6283) * (-1.6283) + 0 = 1.3257.$$

By calculating all of the coefficients, one can obtain the following vector:

$$g = [g_0, g_1, g_2, g_3, g_7, g_5, g_6, g_7, g_8]^T = [1, -1.6283, 1.3257, -1.2099, 1.0914, -1.0240, 0.9525, -0.9067, 0.8570]^T.$$

Now we have all the elements to evaluate the single polynomial by expanding (11) and negating the coefficient of the same power from both sides. Note that $p_0 = 1$

$$P(x) = (-1)^n P(-x) G(1/x)$$

$$p_0 x^4 + p_1 x^3 + p_2 x^2 + p_3 x + p_4 = (p_0 x^4 - p_1 x^3 + p_2 x^2 - p_3 x - p_4)(1 + g_1/x + g_2/x^2 + \dots + g_8/x^8).$$

This leads to the following trapezoidal system:

$$\begin{bmatrix} p_1 \\ p_2 \\ p_3 \\ p_4 \end{bmatrix} = \begin{bmatrix} g_5 & -g_4 & g_3 & -g_2 \\ g_6 & -g_5 & g_4 & -g_3 \\ g_7 & -g_6 & g_5 & -g_4 \\ g_8 & -g_7 & g_6 & -g_5 \end{bmatrix} \begin{bmatrix} g_6 \\ g_7 \\ g_8 \\ g_9 \end{bmatrix} = \begin{bmatrix} -0.8142 \\ -0.6135 \\ 0.4342 \\ 0.0192 \end{bmatrix}.$$

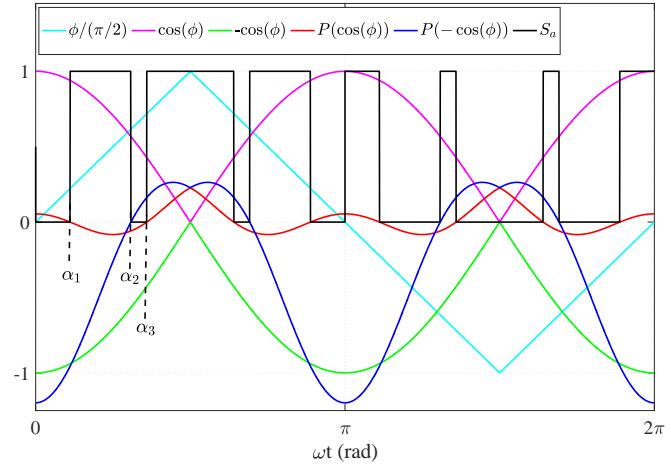


Fig. 3: The zero crossing occurs at the optimal switching angle.

The polynomial is

$$P(x) = x^4 - 0.8142x^3 - 0.6135x^2 + 0.4342x + 0.0192. \quad (21)$$

Now we know how to calculate the polynomial, a novel technique of determining the switching angles from the single polynomial in real-time will be presented in the next section.

C. Obtaining the Optimal Switching Angles

The implementation of the RTSHE can be divided into two routines. A short routine is used when there is a change in the output voltage fundamental frequency, and a longer routine is used when there is a change in either the modulation index, or the number of switching events per fundamental cycle. Typically, under the steady-state conditions, the short routine will be executed. When there is a change in the modulation index, a subroutine to calculate the new polynomial coefficients is triggered as shown in Fig. 2.

First, the reference voltage angles of the three-phase reference voltage are extracted. Then the optimal switching angles are obtained by a simple substitution of $x = \cos(\phi)$ and

$x = -\cos(\phi)$ in $P(x)$, where ϕ is the reference angle of the phase voltage. When the value of the polynomial is equal to zero, a root of the polynomial is detected as shown in Fig. 3. To extract the switching command S_a in real-time, the authors present a technique similar to Descartes' sign rule as shown in the large square in Fig. 2.

The proposed technique allows for obtaining the actuation commands in real-time without the need to solve the roots of the polynomial, which cannot be done in determinate real-time.

There is no need to worry about sorting the optimal switching angles from lower value to larger value. The direct substitution produces the switching angles with the correct order. The solution of the polynomial does not require great computational effort as it is a direct substitution and does not involve an iterative process or initial guessing. Furthermore, the proposed algorithm is valid for multilevel inverters. The only thing that needs to be changed is to use (7) instead of (6) and rearrange the logic in Fig. 2 to provide the switching functions for all of the switches.

The straightforward evaluation of a polynomial using a floating point controller would follow this form: p_0x^n is calculated, then $p_1x^{n-1}, \dots, p_{n-2}x$, and finally all the terms are added. Such a process requires $2n-1$ multiplications and n additions. To optimize this process, one can use Horner's rule to rearrange the computation of the polynomial. Horner's rule requires n multiplications and n additions [21]. Furthermore, there is no need to store the partial results since each quantity arising during the calculation can be used immediately after it has been computed. The computational effort can be further reduced by adaptation of the coefficients [21]. Since the leading coefficient in RTSHE polynomials has the largest value, the division by the leading coefficient will never lead to instability.

III. COMPARISON WITH THE OFFLINE SELECTIVE HARMONIC ELIMINATION

The traditional approach of implementing the selective harmonic elimination method is by solving the transcendental system of equations (2) using an iterative method. Since the solution needs to be evaluated for each possible modulation index, it is more convenient to solve for a limited number of modulation indices and extrapolate the values of the optimal switching angles between every two solutions and store the data in the form of curve fitting polynomials. The interested reader may check [22] where the Newton-Raphson iterative method is used to solve the transcendental equations. As the number of selected harmonics increases, Newton's method becomes more sensitive to the initial conditions. For instance, to achieve convergence for six switching angles per quarter fundamental cycle, one needs to use the solution from the previous few steps instead of the most recent step. The uncertainty of the initial guess along with the indeterminate convergence time, if any, makes the real-time implementation of the transcendental equations an unattractive approach. Since the real-time selective harmonic elimination involves more mathematical processes, it is essential to check the numerical

difference between the real-time solution and the solution obtained by offline calculation. Fig. 4(a) shows the numerical difference of the first three odd harmonic magnitudes of the real-time approach and the offline approach in both 60 Hz and 120 Hz fundamental frequencies. Fig. 4(b) shows similar results when eliminating the first six odd harmonics.

In Fig. 4(a), the value of the third harmonic in the offline approach is larger than the one from the real-time implementation. This due to the inaccuracy of the curve fitting. It can be improved by creating a higher order polynomial to represent the curve. In our case, the order of the curve fitting polynomial is kept equal to the order of the univalent polynomial of the real-time implementation. The norm of residuals along with other error-contributing factors are quantified in Table I. Fig. 5 shows the total harmonic content divided by the fundamental component. This number does not change when n is increased from 4 to 6 to 8,..., etc. The benefit of increasing n is that all of the harmonics concentration will be located to the right of the last eliminated harmonic. This result in harmonic content with higher frequency. Therefore, the current resulting from these harmonic will have less amplitude due to the inductive nature of the load impedance ($Z_L = 2\pi fL$). Furthermore, it is important to note that the total harmonic content is exactly the same as the one produced by the offline SHE.

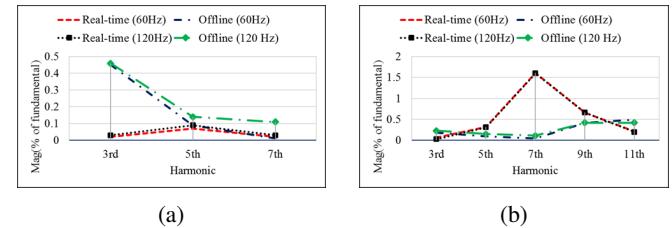


Fig. 4: Numerical results show a comparison between the eliminated harmonics magnitudes of the proposed real-time method and of the conventional offline method when (a) eliminating the first three odd harmonics and (b) eliminating the first five

odd harmonics. Both figures show the results in two fundamental frequencies 60 Hz and 120 Hz.

IV. SELECTIVE HARMONIC MODULATION

So far the intent behind implementing the RTSHE is to achieve a desired modulation index and to eliminate the lower order harmonics. In this section, we show that the proposed RTSHE can be generalized such that the lower order harmonics can have any arbitrary value rather than zero. Hence the generalized method is called the real-time selective harmonic modulation RTSHM.

Starting from the system of algebraic polynomials in (3), $s_1, s_3, \dots, s_{2n-1}$ can be obtained using the proposed recursive algorithm:

$$T_{2n-1}(x)|_{(x^{2n-1}=s_{2n-1})} = \frac{1}{2} + \frac{n\pi b_{2n-1}}{8V_{dc}}. \quad (22)$$

To better understand the proposed algorithm, we apply it to the earlier example: for that matter the modulation index

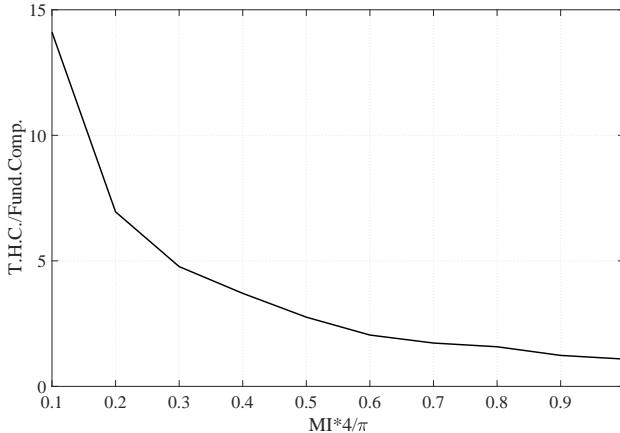


Fig. 5: Total harmonic content divided by the fundamental component for both the offline SHE and the proposed real-time SHE. Note that this number does not change by changing the number of eliminated harmonics, instead, the harmonics get shifted to the right of the last eliminated harmonic and this result in a better load current performance. This is due to the fact that higher-frequency harmonics face higher impedance in an inductive load.

is kept at 0.6283 and the third harmonic $b_3 = 0.2$. The substitution of the Chebyshev's first polynomial ($T_1 = x$) in (22) yields

$$s_1 = \frac{1}{2} + \frac{\pi b_1}{8V_{dc}}.$$

Similarly, the substitution of Chebyshev's third polynomial ($T_3 = 4x^3 - 3x$) in (22) yields

$$\begin{aligned} 4s_3 - 3s_1 &= \frac{1}{2} + \frac{3\pi b_3}{8V_{dc}} \\ s_3 &= \frac{3s_1}{4} + \frac{3\pi b_3}{32V_{dc}} + \frac{1}{8} \end{aligned}$$

and

$$\begin{aligned} s_5 &= \frac{5s_3}{4} - \frac{5s_1}{16} + \frac{5\pi b_5}{128V_{dc}} + \frac{1}{32} \\ s_7 &= \frac{7s_1}{64} - \frac{7s_3}{8} + \frac{7s_5}{4} + \frac{7\pi b_7}{512V_{dc}} + \frac{1}{128}. \end{aligned}$$

As it can be seen, the value of s in (6) is only dependent on the value of b_1 while in (22) it is dependent on the value of each harmonic including b_1 . Therefore, we can assign any value to any harmonic and the rest of the algorithm, remains unchanged. Note that if the modulation of several harmonics is needed to be implemented using the offline approach, with each modulated harmonic, the size of the look-up table will be doubled. This makes it impossible to solve and store within the limited memory of the microcontroller.

V. EXPERIMENTAL RESULTS

Experimental tests have been performed to validate the efficacy of the proposed method. The three-phase, two-level voltage source inverter shown in Fig. 1 is used. The DC-link voltage is $V_{dc} = 100$ V. The motor is replaced with

equivalent RL load $R = 5 \Omega$ and $L = 2 \text{ mH}$. The controller used in the experiment is dSPACE CP1103. The digital output pins were used to generate the switching signals. Therefore, the calculations of the algorithm are done by the dSPACE PowerPC PCC 750GX and Xilinx Spartan 6 FPGA.

The first test is conducted to investigate the effect of the sampling frequency on the accuracy of the generated switching signals. The RTSHE algorithm was set to calculate the new polynomial coefficients and substitute the value of the reference voltage angle into the new polynomial (long routine). Since the algorithm requires approximately $6 \mu\text{s}$, the fixed sampling time is set to $8 \mu\text{s}$. Fig. 6(a) and (b) show a comparison between the waveforms resulting from the real-time algorithm and the waveforms resulting from using the offline method. Note that the offline method uses a curve fitting polynomial to obtain the optimal switching angle. The order of the curve fitting polynomial is set to the same order as the polynomial in the real-time algorithm. The offline method requires approximately $4 \mu\text{s}$ turnaround time. For comparison, the fixed sampling frequency for the offline method is also set to $8 \mu\text{s}$. The experimental waveform shows that the value of the eliminated harmonics is still very close to zero. This is justifiable because at 60 Hz frequency, it takes 0.0167 s to complete one cycle. An update for the switching angle can be made by the controller every $8 \mu\text{s}$. This leads to 2087 updates per fundamental cycle. Therefore, the error of the generated switching angle cannot be larger than ± 0.172 degrees. Fig. 7(a) and (b) show similar results when the fundamental frequency is set to 120 Hz. In this case, the error of the switching angles of the real-time method is bounded by ± 0.345 degrees. Slight difference in the spectrum can be observed at the frequencies beyond the eliminated harmonics on the right side of the FFT window.

Fig. 8(a) and (b) show the steady-state performance of the proposed RTSHE method when the fundamental frequency is 60 Hz and 120 Hz, respectively, and the first eight odd harmonics are eliminated. It is clear from the FFT results that the first seven odd harmonics are successfully eliminated for both cases.

Fig. 9(a) shows the transient behavior of the RTSHE method when the switching frequency of the system is changed from 32 Hz to 16 Hz. Fig. 9(b) shows the transient behavior when M_i is increased from 0.6 to 0.8. Fig. 9(c) shows the transient behavior when the inverter reduces the switching frequency and concurrently increases the fundamental frequency. This is very common in high power inverters when the high power GTOs are only able to switch at a rate less than 100 Hz. The load current shows a seamless transition in all of these cases. The concurrent change in the fundamental and switching frequencies is tested at random instants within the fundamental period to inspect any possible current spikes. As shown in Fig. 10(a), (b), and (c), no current spike was ever observed. For comparison, the current transient behavior of the conventional offline method is shown in Fig. 11(a), (b), and (c).

Fig. 12(a) to (c) demonstrate the ability to achieve control over the third harmonic without affecting the fundamental component of the phase voltage and the THD of the load current.

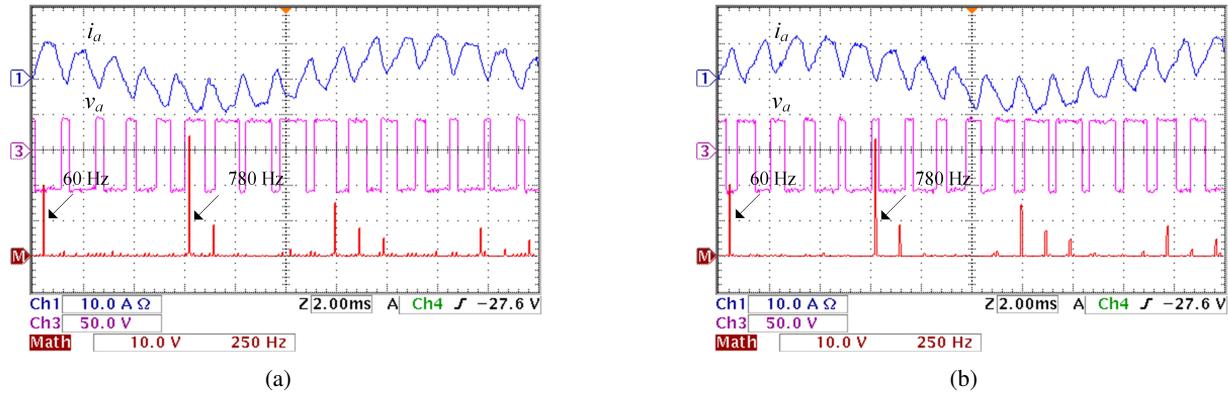


Fig. 6: Experimental results of the line current i_a , line-neutral voltage v_a , and the spectrum of v_a using (a) the proposed real-time algorithm and (b) the conventional offline method. The fundamental frequency for both cases is 60 Hz.

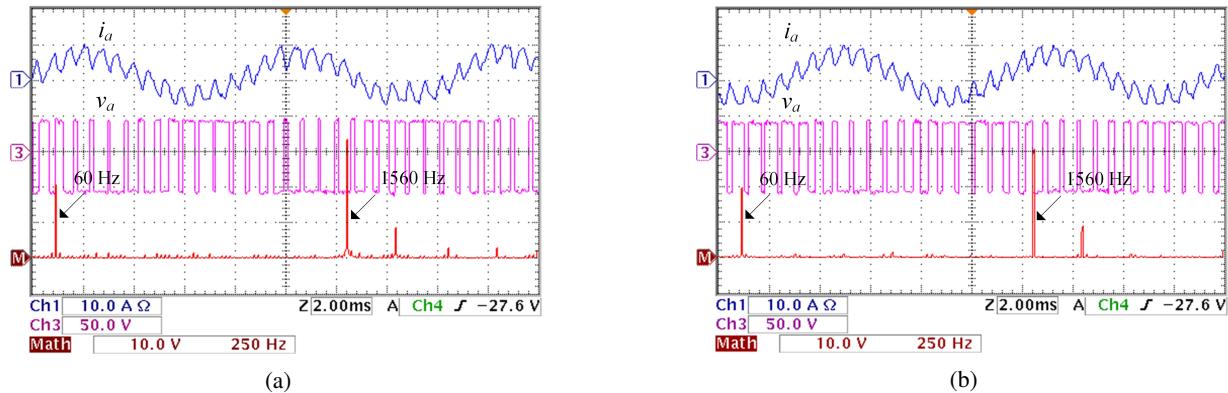


Fig. 7: Experimental results of the line current i_a , line-neutral voltage v_a , and the spectrum of v_a using (a) the proposed real-time algorithm and (b) the conventional offline method. The fundamental frequency for both cases is 120 Hz.

To further reduce the execution effort, the coefficients of the polynomial can be pre-calculated and hard-coded in the controller. To have the flexibility to operate at any M_i , the algorithm that calculates the polynomial coefficient needs to be executed by the controller in real-time. Note that this is required only when the M_i changes. The execution time of the control algorithm only takes $6 \mu\text{s}$, which leaves ample room to increase the system fundamental frequency while maintaining high-quality waveforms. Furthermore, the calculation of the polynomial and the actuation command extraction can be done by the external FPGA, especially when the order of the polynomial is large. Using an external FPGA allows parallel schemes for software realization, and based on the number of the available parallel units, the overall turnaround time can be further reduced [23].

VI. CONCLUSION

In this paper, a new real-time SHE implementation method is presented. By the transformation of variables, the transcendental equations of the optimization problem are converted to a set of algebraic equations using Chebyshev polynomials. Then the set of algebraic equations is reduced to a single univalent polynomial using generalized Newton's identities. The roots of this polynomial hold the values of the switching angles. The switching angles are calculated in real-time by simple

substitution of the reference phase. The original contributions of the proposed RTSHE/M are the following:

- 1- Presenting the generalized Chudnovsky algorithm. The new algorithm allows modulating the selected harmonics rather than only eliminating them. In the near future, this feature will be utilized for the wireless energy transfer of the multi-receiver case.
- 2- Presenting a new method of obtaining the values of the optimal switching angles from the polynomial in real-time without resorting to any iterations or guesses. This enabled the implementation in the microcontroller with a determinate execution time.

The proposed method requires minimal computational effort by the controller because it is not an iterative process and does not involve any guessing of initial conditions. Hardware experiments show the superior dynamic performance of the proposed method during a change in the modulation index, switching frequency, and both switching and fundamental frequencies. The proposed method has the efficacy to be a viable replacement for the offline approach and the existing online approaches.

REFERENCES

- [1] A. Janabi and B. Wang, "Real-time implementation of selective harmonic elimination with seamless dynamic performance," 2018 IEEE Energy

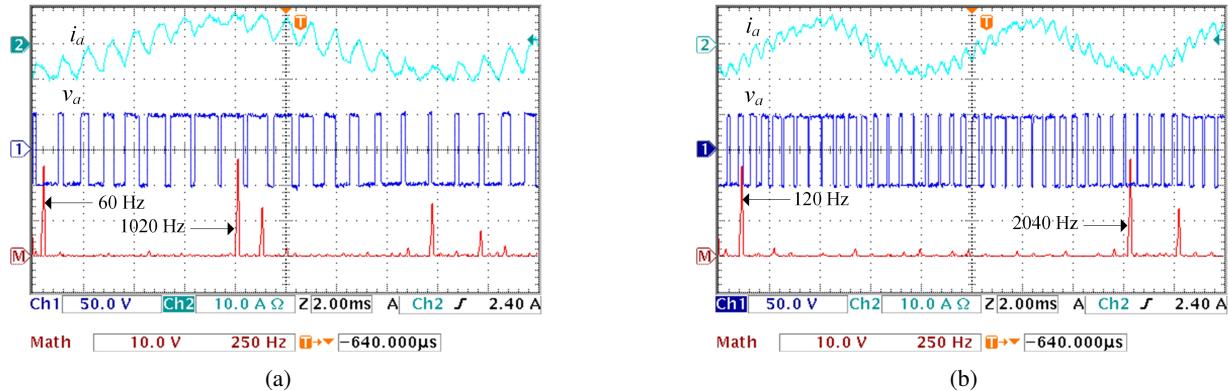


Fig. 8: Experimental results of RTSHE load current i_a and the phase voltage v_a at (a) the fundamental frequency of 60 Hz, and (b) the fundamental frequency of 120 Hz.

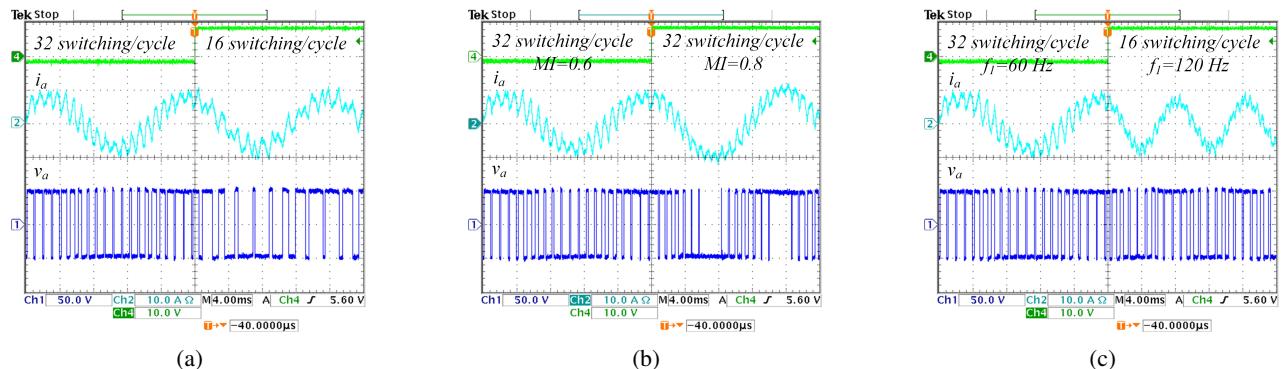


Fig. 9: The transient behavior of the load current i_a and the phase voltage v_a when (a) changing the switching frequency, (b) changing M_i , and (c) changing both fundamental and switching frequencies at the same instant.

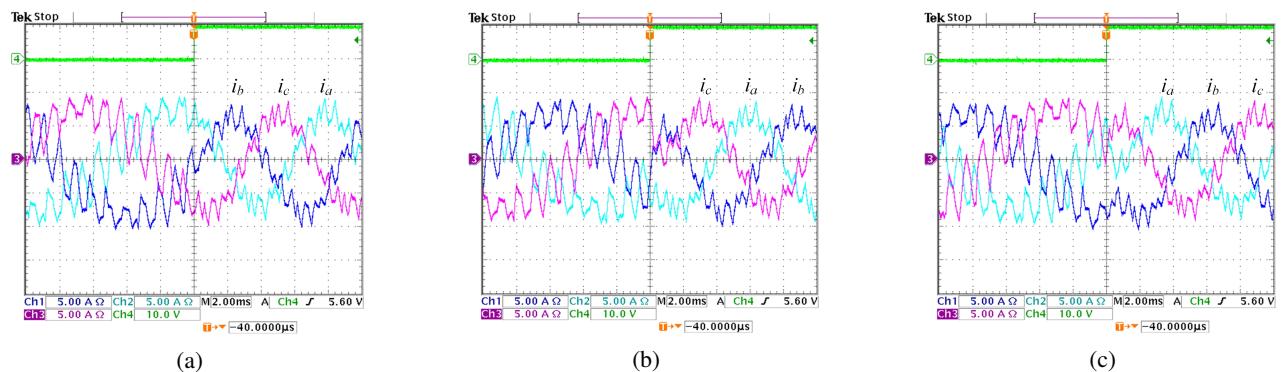


Fig. 10: The transient behavior of the proposed RTSHE load currents i_a , i_b , and i_c when a concurrent change in the fundamental and switching frequencies are randomly requested. No current spike is detected.

- Conversion Congress and Exposition (ECCE), Portland, OR, 2018*, pp. 3362-3366.

 - [2] H. S. Patel and R. G. Hoft, "Generalized techniques of harmonic elimination and voltage control in thyristor inverters: part I-harmonic elimination," in *IEEE Transactions on Industry Applications*, vol. IA-9, no. 3, pp. 310-317, May 1973.
 - [3] M. S. A. Dahidah, G. Konstantinou and V. G. Agelidis, "A review of multilevel selective harmonic elimination PWM: formulations, solving algorithms, implementation and applications," in *IEEE Transactions on Power Electronics*, vol. 30, no. 8, pp. 4091-4106, Aug. 2015.
 - [4] G. Konstantinou, V. G. Agelidis and J. Pou, "Theoretical considerations for single-phase interleaved converters operated with SHE-PWM," in *IEEE Transactions on Power Electronics*, vol. 29, no. 10, pp. 5124-5128, Oct. 1 2014.
 - [5] K. Yang et al., "Unified selective harmonic elimination for multilevel converters," in *IEEE Transactions on Power Electronics*, vol. 32, no. 2, pp. 1579-1590, Feb. 2017.
 - [6] Z. B. Duranay and H. Guldemir, "Selective harmonic eliminated V/f speed control of single-phase induction motor," in *IET Power Electronics*, vol. 11, no. 3, pp. 477-483, 3 20 2018.
 - [7] J. Holtz and N. Oikonomou, "Synchronous optimal pulselwidth modulation and stator flux trajectory control for medium-voltage drives," in *IEEE Transactions on Industry Applications*, vol. 43, no. 2, pp. 600-608, March-april 2007.
 - [8] J. Holtz and B. Beyer, "The trajectory tracking approach-a new method for minimum distortion PWM in dynamic high-power drives," in *IEEE Transactions on Industry Applications*, vol. 30, no. 4, pp. 1048-1057, Jul/Aug 1994.

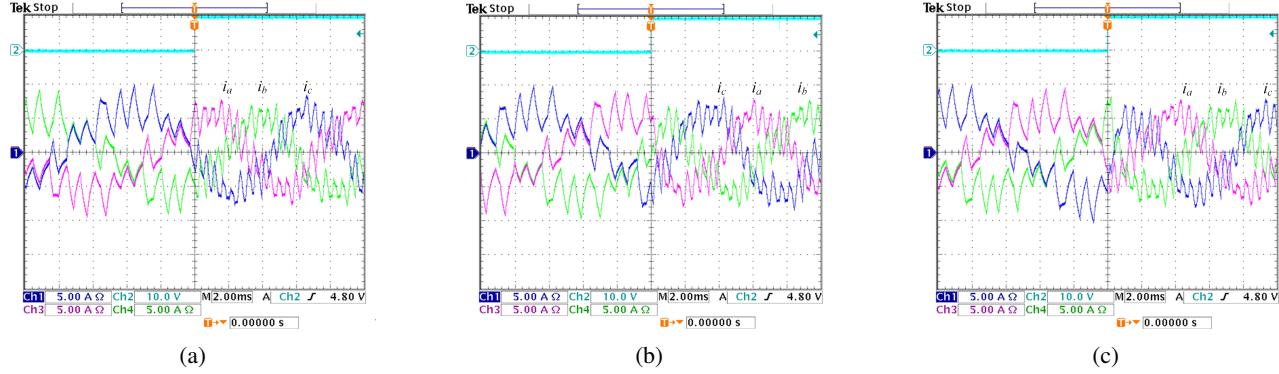


Fig. 11: The transient behavior of the conventional offline SHE load currents i_a , i_b , and i_c when a concurrent change in the fundamental and switching frequencies are randomly requested.

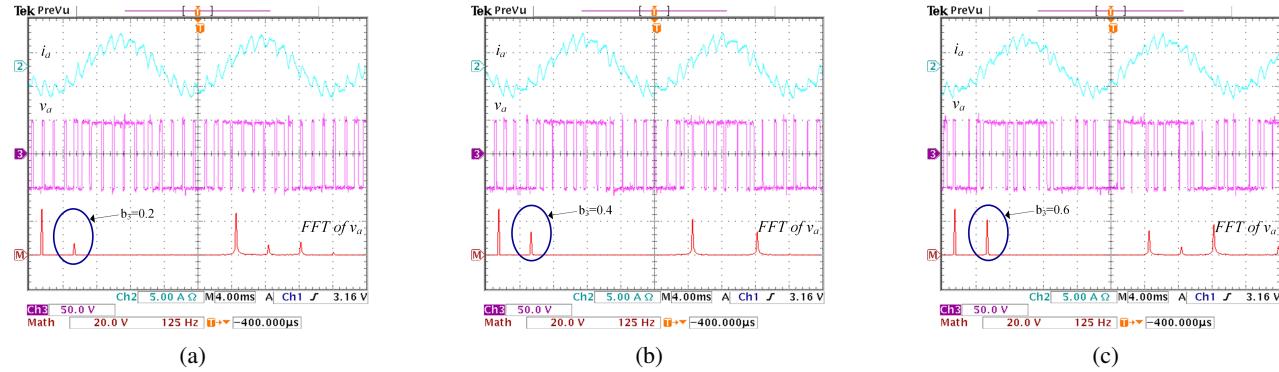


Fig. 12: The real-time controllability of the third harmonic: (a) $v_{b3} = \frac{\pi b_3}{4} * V_{dc}/2 = \frac{\pi 0.2}{4} * 50 = 7.855$ V, (b) $v_{b3} = \frac{\pi b_3}{4} * V_{dc}/2 = \frac{\pi 0.4}{4} * 50 = 15.71$ V, and (c) $v_{b3} = \frac{\pi b_3}{4} * V_{dc}/2 = \frac{\pi 0.6}{4} * 50 = 23.565$ V.

TABLE I: Summary of the comparison between the conventional offline method and the proposed RTSHE/M.

Trade	Conventional Offline Method	Proposed RTSHE/M
Error Due Numerical Conv.	$\approx 10^{-15}$	$\approx 10^{-15}$
Error Due Implementation	Norm of residuals = 0.076104	No implementation error
Error Due Sampling	0.08 degrees; proportional to the fundamental frequency and n	0.172 degrees; proportional to the fundamental frequency and n
Offline Complexity	Requires solving difficult mixed integer programming problem, especially when n is large.	No offline solution required.
Online Complexity	Minimal	The additional calculation almost doubles the turnaround time compared to the offline method.
Transient Behavior	May undergo high current transient when transferring from a set of angles to another due to change in M_i .	Improved due to the high achievable M_i precision.
Ability to Remove the Selected Harmonics	Able to remove the selected harmonics. THD is the same as the one from the offline method.	Able to remove the selected harmonics. THD is the same as the one from the offline method.

- [9] Y. Liu, H. Hong and A. Q. Huang, "Real-time calculation of switching angles minimizing THD for multilevel inverters with step modulation," in *IEEE Transactions on Industrial Electronics*, vol. 56, no. 2, pp. 285-293, Feb. 2009.
- [10] M. Ahmed, A. Sheir and M. Orabi, "Real-time solution and implementation of selective harmonic elimination of seven-level multilevel inverter," in *IEEE Journal of Emerging and Selected Topics in Power Electronics*, vol. 5, no. 4, pp. 1700-1709, Dec. 2017.
- [11] J. R. Wells, X. Geng, P. L. Chapman, P. T. Krein and B. M. Nee, "Modulation-based harmonic elimination," in *IEEE Transactions on Power Electronics*, vol. 22, no. 1, pp. 336-340, Jan. 2007.
- [12] C. Buccella, C. Cecati, M. G. Cimoroni and K. Razi, "analytical method for pattern generation in Five-level cascaded H-bridge inverter using selective harmonic elimination," in *IEEE Transactions on Industrial Electronics*, vol. 61, no. 11, pp. 5811-5819, Nov. 2014.
- [13] Jian Sun, S. Beineke and H. Grotstollen, "Optimal PWM based on real-time solution of harmonic elimination equations," in *IEEE Transactions on Power Electronics*, vol. 11, no. 4, pp. 612-621, Jul 1996.
- [14] H. Patangia and S. Bhadra, "Design equations for selective harmonic elimination and microcontroller implementation," *IECON 2014 - 40th Annual Conference of the IEEE Industrial Electronics Society*, Dallas, TX, 2014, pp. 1391-1396.
- [15] Tables of Chebyshev Polynomials. Washington: U.S. Govt. Print. Off., 1952.
- [16] Nabae, Akira, Isao Takahashi and Hirofumi Akagi. "A new neutral-point-clamped PWM inverter." *IEEE Transactions on Industry Applications IA-17* (1980): 518-523.
- [17] D. Czarkowski, D. V. Chudnovsky and I. W. Selesnick, "Solving the optimal PWM problem for single-phase inverters," in *IEEE Transactions on Circuits and Systems I: Fundamental Theory and Applications*, vol.

- 49, no. 4, pp. 465-475, Apr 2002.
- [18] Chudnovsky, D. V. and G. V. Chudnovsky. "Solution of the pulse width modulation problem using orthogonal polynomials and Korteweg-de Vries equations." *Proceedings of the National Academy of Sciences of the United States of America* 96 22 (1999): 12263-8 .
- [19] Ronald L. Graham, Donald E. Knuth, and Oren Patashnik. 1989. "Concrete mathematics: a foundation for computer science." *Addison-Wesley Longman Publishing Co., Inc., Boston, MA, USA*.
- [20] Leonhard Euler; J. D. Blanton (transl.) (1988). "Introduction to analysis of the infinite", Book 1. *Springer. ISBN 978-0-387-96824-7*.
- [21] D. E. Knuth, *The art of computer programming*. New York: Addison-Wesley, 1981, vol. 2.
- [22] D. Grahame Holmes; Thomas A. Lipo,"Programmed modulation strategies," in Pulse Width Modulation for Power Converters:Principles and Practice , 1, *Wiley-IEEE Press*, 2003, pp.744-
- [23] Xu, Simin and Wei Ting Loke."efficient polynomial evaluation algorithm and implementation on FPGA." (2013).